Journal of Molecular Liquids 337 (2021) 116206

Contents lists available at ScienceDirect

Journal of Molecular Liquids

journal homepage: www.elsevier.com/locate/molliq

Styrene intermolecular associating incorporated-polyacrylamide flooding of crude oil in carbonate coated micromodel system at high temperature, high salinity condition: Rheology, wettability alteration, recovery mechanisms

A. Maghsoudian [a], Y. Tamsilian [b], S. Kord [a], B. Soltani Soulgani [a], A. Esfandiarian [a], M. Shajirat [a]

[a] Department of Petroleum Engineering, Ahvaz Faculty of Petroleum, Petroleum University of Technology, Ahvaz, Iran
[b] Department of Chemical Engineering, Faculty of Engineering, Shahid Chamran University of Ahvaz, Ahvaz, Iran

ARTICLE INFO

Article history:
Received 20 January 2021
Revised 25 March 2021
Accepted 16 April 2021
Available online 20 April 2021

Keywords:
Enhanced oil recovery
Hydrophobically associating polymer
High temperature and high salinity
Viscosifying
Wettability alteration
Interfacial tension

ABSTRACT

Polymer flooding is one of the most well-known research interests in the enhanced oil recovery (EOR) due to the excess oil production and limited petroleum reserve. Commercial polymers such as polyacrylamide (PAM) and its hydrolyzed form (HPAM) can be easily degraded at high temperature, high salinity, and high shear rate in attempt to the EOR purposes for the harsh reservoir conditions. In this work, a hydrophobically modified copolymer consisting of acrylamide and styrene (HSPAM) was produced via inverse emulsion polymerization as a wettability modifier and viscosifying agent, applicable under harsh reservoir conditions to direct insights into the synergic oil recovery pore scale mechanisms and overcoming the aforementioned challenges through the EOR process. In the first part of this study, a set of analytical techniques including FTIR, NMR, TGA, and molecular weight measurement was carried out, confirming successfully incorporation of styrene monomer in water-soluble skeleton and higher thermal resistivity of HSPAM compared with HPAM. By analyzing the rheological behavior of HSPAM under harsh reservoir conditions, it was found that the viscosity of HSPAM aqueous solution was increasingly influenced by the total dissolved solids, even up to 40,572 mg/L. In the second part, stability tests, contact angle (CA), interfacial tension (IFT), and carbonate coated glass micromodel flooding experiments were conducted by deionized water (DIW), seawater (SW) and formation brine (FB) in the absence and presence of HSPAM and HPAM. HSPAM illustrated a great stability in seawater and formation brine in comparison with HPAM after 120 days at 80 °C. The presence of HSPAM in seawater resulted in a more water-wet state up to 42° compared to HPAM by contact angle of 31° after 72 h. Findings provided synergic oil recovery mechanisms approved by emulsification and coalition phenomena to show a better wettability alteration and IFT reduction for HSPAM in spite of HPAM alongside drastically improving the brine-based flooding performance, yielding an ultimate recovery of about 82% original oil in place (OOIP).

1. Introduction

Through the decline in oil productions in recent decades, the importance of oil recovery improvement has been increased. Therefore, finding an appropriate method to enhance oil recovery (EOR) is one of the most vital steps in oilfield master development plans [1,2]. The sweep efficiency of water flooding (secondary oil recovery stage), as one of the widely used oil recovery processes, is not significant because of the high water cut in some hydrocarbon reservoirs [3–5]. Governing harsh conditions such as fractured, vugular, high temperature, high salinity (HTHS) and approximately oil-wet as well as numerous oil displacing mechanisms are the main challenges in the carbonated reservoirs for more than 60% of the oil and gas reservoirs [6]. These limitations resulted in obtaining the lower oil recovery factors from the carbonate reservoirs than those of sandstones [7,8]. Therefore, this obstacle opens a great opportunity to conduct precise experimental tests for finding the best method to increase the ultimate oil recovery.

As an alternative commercial method, the polymer flooding, including aqueous solutions of high molecular weight polyacrylamide (PAM) and its partially hydrolyzed form (HPAM), is an appropriate candidate for improving recovery factor through increasing volumetric sweep efficiency up to 5–30% original oil in

E-mail addresses: tamsilian@scu.ac.ir (Y. Tamsilian), sh.kord@put.ac.ir (S. Kord), soltani.b@put.ac.ir (B. Soltani Soulgani)

https://doi.org/10.1016/j.molliq.2021.116206
0167-7322/

place (OOIP%), which is the result of the polymer conformance control technique and water phase viscosity enhancement [9–13]. A wide variety of different commercial polymers have been suggested in the field of the polymer flooding utilization for sandstone reservoirs [14–17], but there are limited industrial and laboratory experiences for the polymer injection in the carbonated reservoirs due to the harsh environment conditions [10,14,18]. On the other hand, applying conventional polymers in the chemical EOR (CEOR) processes encounters some constraints including chemical, thermal, mechanical, and biological degradation as well as surface adsorption of polymer chains during the flooding process [18–21]. Expressly, the high amount of monovalent and divalent cations such as Na^+, Ca^{2+}, and Mg^{2+} in the saline water displacing fluid and reservoir temperature strongly affect the polymer chain degradation and extremely decrease the viscosity of the polymer solution during the flooding process [22,23]. Hitherto, numerous researches have been performed to copolymerize the acrylamide, a common water-soluble polymer for EOR, with a suitable moiety in attempt to overcome the disadvantages of the conventional polymers and to provide a good performance in both sandstone and carbonated reservoirs [24–29]. The main focus of these studies has been on replacing several AM moieties in the main chain with higher resistance monomers [30,31]. Star-shaped polymer [32], comb-shaped polymer [33], poly(acrylamide and vinyl pyrrolidone) [34], poly(acrylamide and 2-acrylamide 2-methyl propane sulfonate) [34,35], and poly(acrylamide and styrene) [29] are some examples for the high salinity and temperature tolerated copolymers produced for the EOR purposes. However, their industrial aspects have not been really explored enough and only a few experiences are commercially available for the copolymers. Thus, designing and developing novel, cost-effective and simple polymers are essential to be easily applied into the specific oil production approach. Hydrophobically associative copolymers have been developed as strong, effective, resilient, flexible, highly resistant and low-price products [36–39]. These polymers including a wide range of compounds with different functional groups and properties can recover higher amounts of oil and displace a large portion of by-passed oil [40]. Hydrophobically modified water-soluble polymers (HMP) contain a slight amount of hydrophobic groups attached to the water-soluble polymer backbone [41]. The main goal of synthesizing HMPs is to participate in the intermolecular association to enhance the displacing fluid viscosity in harsh reservoir conditions [42]. This polymeric category has been a subject of interest in recent decades due to their unique structures and features like the thickening properties, shear-thinning, and rheology-modifying behavior [6,18,41,43,44]. The great potential of impacting on reservoir mechanisms such as wettability alteration (WA) [45,46], pH effect [40], IFT reduction [47,48], and better response against the reservoir heterogeneity [49,50] compared to conventional polymers make them a suitable candidate for HTHS reservoir conditions [51]. In return, this approach has been limited by complex synthesis procedures, expensive and toxic initial materials in the most cases [43,52]. Among the hydrophobic monomers, the considerable researches have been devoted to styrene due to easy accessibility, appropriate conformational freedom, less toxicity, excellent viscosity, and cost-effective material to incorporate in the copolymer structures to improve the performance [52–57]. To simplify the copolymerization and overcome the disadvantages of the classical polymers through CEOR, Tamsilian et al. worked on nanostructured particles for the controlled polymer release. They designed a core-shell nanostructure for protecting acrylamide polymer by polystyrene, called PPN, to resist in the harsh reservoir condition. The obtained results showed that the use of polystyrene included in the core-shell increased the stability of PAM at the high temperature and salinity as well as vigorous shear rate conditions in comparison with the conventional polymers [58]. In the following, Shaban et al. conducted a set of characterization tests to investigate the styrene effects in the acrylamide-styrene copolymer using the aerosol copolymerization. They illustrated that the aerosol method led to produce highly pure copolymers, no required to use the surfactants for the copolymerization [37]. Khakpour et al. synthesized acrylamide-styrene copolymers using the micellar copolymerization method and sodium dodecyl sulfate (SDS) surfactant to characterize the copolymer microstructure. Their observed results from the micellar method showed that a higher mole fraction of styrene could participate in the copolymer [59]. Lalegani et al. found that the styrene monomer participation in the main structure of poly (acrylamide-maleic acid-styrene) should be less than 10 percent in order to the fully water solubility [29]. In the following, Antoniv et al. performed a surfactant-free emulsion radical polymerization to synthesize the poly(styrene-co-acrylamide) which was led to a smaller average particle size, appropriate particle size distribution, and lower molecular weight distribution compared to the previous synthesis procedures [60].

Previous studies demonstrated styrene modified water-soluble polymer had an appropriate stability in harsh reservoir conditions such as the shear-resistance and the salt-resistance properties of the solutions progressed by applying the styrene hydrophobic units in hydrophilic polymer structure [61]. To the best of our knowledge, direct insights into the synergic oil recovery pore scale mechanisms – viscosifying, wettability alteration, IFT reduction, effect of reservoir heterogeneity – by the hydrophobically styrene modified polyacrylamide flooding of crude oil through the HTHS carbonate reservoirs are the main gap in the literatures. In this work, the synergistic effect of seawater and a novel styrene intermolecular associating incorporated-polyacrylamide, HSPAM, was investigated with the purpose of solving the classical polymer flooding challenges and making a drastic improvement in the oil sweep efficiency to propose an excellent candidate for the EOR applications. This associating polymer with the advantages of viscosifying and wettability modifying offered a great stability in harsh reservoir conditions compared to the similar chemicals. In the first part of this study, HSPAM was synthesized by inverse emulsion polymerization of acrylamide and styrene to incorporate short-chain hydrophobic blocks through the hydrophilic backbone. Next, a set of analytical techniques, thermal analysis, and rheology measurement was conducted to confirm the incorporation of styrene monomer in the polymer chain and characterize the produced copolymer under harsh reservoir conditions. Finally, stability tests, the wettability alteration and IFT measurements alongside flooding experiments in a carbonate coated micromodel were performed in both absence and presence of the polymers. Fig. 1 demonstrates the experimental procedure considered in this study.

2. Materials and methodology

2.1. Materials

Acrylamide (AM, 99.0%), styrene (99.9%), azobisisobutyronitrile (AIBN, 99.9%), and toluene (99.6%) were provided from Merck Company (Germany). Monooleate Span80 emulsifier with a hydrophilic-lipophilic balance (HLB) of 4.3 was used without any further purification. Double distilled water used for preparing the water in oil emulsion, was deprived of oxygen by heating to the boiling point and cooling under the stream of nitrogen. As two comparative commercial polymers, non-hydrolyzed polyacrylamide (PAM) for characterization tests and 30% hydrolyzed polyacrylamide (HPAM3340) for the rheology properties and EOR analysis with molecular weights of 8×10^6 and 1.2×10^6 g/mol, were selected, respectively.

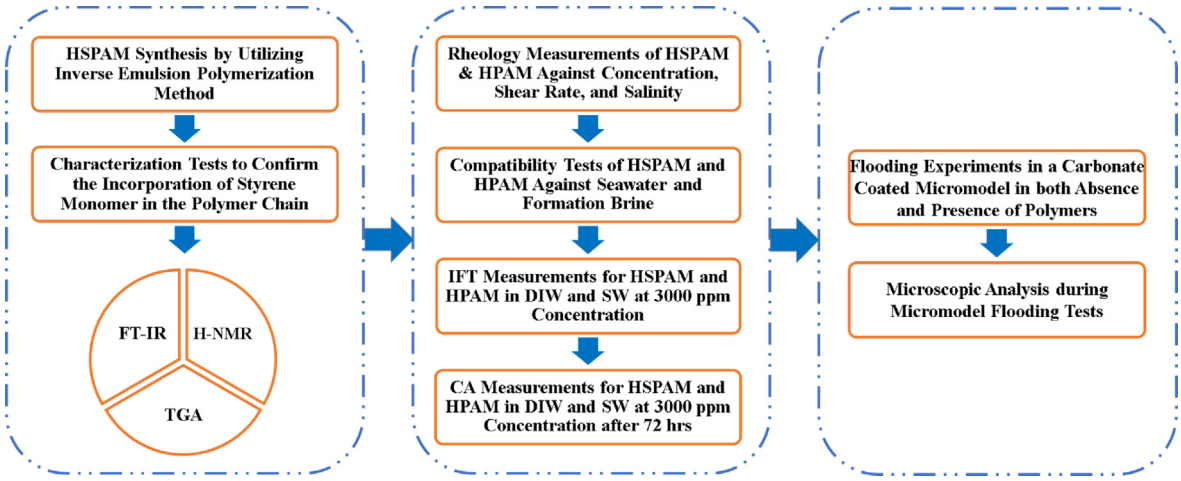

Fig. 1. Experimental procedure considered in this study.

The crude oil sample extracted from one of the southern Iranian carbonated oilfields was filtered by applying 5 μm filtration paper to obliterate the solid particles. The oil properties and saturate, aromatic, resin, asphaltene (SARA) analysis of the crude oil are illustrated in Table 1 [62].

To prepare seawater (SW) and formation brine (FB) with the total dissolved solids (TDS) of 40,572 and 195,475 ppm, six different types of salts including NaCl, KCl, $CaCl_2$, $MgCl_2$-$6H_2O$, Na_2SO_4, $NaHCO_3$ purchased from Merck company (Kenilworth, England, 99% purity) were used and dissolved in deionized water (DIW) [62]. Brine composition and values for the mentioned synthetic SW (40,572 ppm) and formation brine (FB) (195,475 ppm) applied for the stability tests are shown in Table 2.

2.2. Polymerization procedure

In this study, the acrylamide-based polymer incorporated with hydrophobic styrene was designed and produced by a one-pot inverse emulsion polymerization [61,63]. Dissolved acrylamide (0.65 M) in a NaCl aqueous solution (2.58 M) was homogenized into a mixture of toluene (7.35 M) and monooleate Span80 emulsifier (0.04 M) for 40 min under the maximum homogenizer speed and inert gas purging. After the complete emulsification in the reactor, styrene hydrophobic monomer (0.07 M to the continuous phase) and AIBN hydrophobic initiator (0.009 M to the continuous phase) were gradually mixed in the reactor recipe to start the polymerization process at the constant setting to 62 °C and 220 rpm for 240 min. Finally, the milky HSPAM emulsion was precipitated and washed in the high amount of ethanol (1:5) to remove the impurities. After the ethanol evaporation, the pure product was dried in an oven for 1 week at 50 °C to evaporate the remained water. Fig. 2 shows the schematic of the polymer synthesis procedure.

Table 1
Crude oil properties.

Properties	Value	Unit
Density	0.87	gr/mL
API	33.03	–
Viscosity	40.28	mPa.s
Saturates	49.2	wt%
Aromatics	37.6	wt%
Resins	8.1	wt%
Asphaltene	4.6	wt%

2.3. Characterizations and rheology analysis

A set of analytical techniques including FTIR and ^{1}H NMR combining with thermo-gravimetric analysis (TGA), molecular weight test, and rheology measurements in the harsh environment were implemented to examine the HSPAM structure and analyze the incorporation of styrene monomer in the polymer chain.

The quality of synthesized HSPAM was investigated using ATR-FTIR and ^{1}H NMR techniques. FTIR spectra wavenumber was conducted between 400 and 4000 cm^{-1} by Bruker Tensor II device made by Germany. For ^{1}H NMR test, the synthesized polymer was dissolved in deuterium (D_2O) to be analyzed by ^{1}H NMR Bruker 400 MHz spectroscopy (Germany). Refer to the insolubility of polystyrene in D_2O, neat polystyrene was not discovered by ^{1}H NMR and only styrene units embedded in the polymer backbone could be represented.

For the associating polymer, it was assumed that there are Y units of hydrophobic styrene monomer and X units of hydrophilic acrylamide monomer per 100 monomer units. By using the ^{1}H NMR result and Eqs. (1) and (2), the percentage of styrene monomer was calculated [37].

$$Y\% = \frac{3S_c}{5(S_a + S_b)} \times 100\% \quad (1)$$

$$Y\% + X\% = 100\% \quad (2)$$

where S_c is the integrating area of a proton from the benzene ring, S_a and S_b are attributed to the integrating area of protons from the aliphatic group (—CH_2—) and (—CH—), respectively.

The thermo-gravimetric analysis was also applied to investigate the thermal degradation behavior of PAM and HSPAM in the range of 50–600 °C by Simultaneous Thermal Analysis (PT 1600, LINSEIS, Germany) under the nitrogen atmosphere. The descending trend of the diagram revealed that the sample mass dwindling was completely affected by the temperature increase.

Ubbelohde capillary viscometer (constant factor = 0.003 mm^2/s^2) was used to determine the final value of the reduced viscosity and effect of polymer concentration on the HSPAM behavior [29]. Based on Eq. (3), η, M, k, and a are the intrinsic viscosity, molecular weight, and constants in Mark-Houwink equation, respectively. This equation is an appropriate method to calculate the molecular weight at room temperature. Constant parameters in Mark-Houwink equation were 6.31×10^{-3} and 0.8 for polyacrylamide and deionized water as a solvent, respectively [37,59]. It was important to mention that this method was an approximate

Table 2
Brine composition in synthetic seawater (SW) and formation brine (FB).

Brines	Na^+ (ppm)	K^+ (ppm)	Cl^- (ppm)	Mg^{2+} (ppm)	Ca^{2+} (ppm)	SO_4^{2-} (ppm)	HCO_3^- (ppm)	Concentration (ppm)	pH	Ionic Strength (mmol/l)	Density (g/mL)
FB	72,698	303	115,375	585	5,950	168	396.50	195,475	7.3	6,446	1.1106
SW	12,290	280	22,652	1,530	460	3,210	122	40,572	8	1,291	1.0053

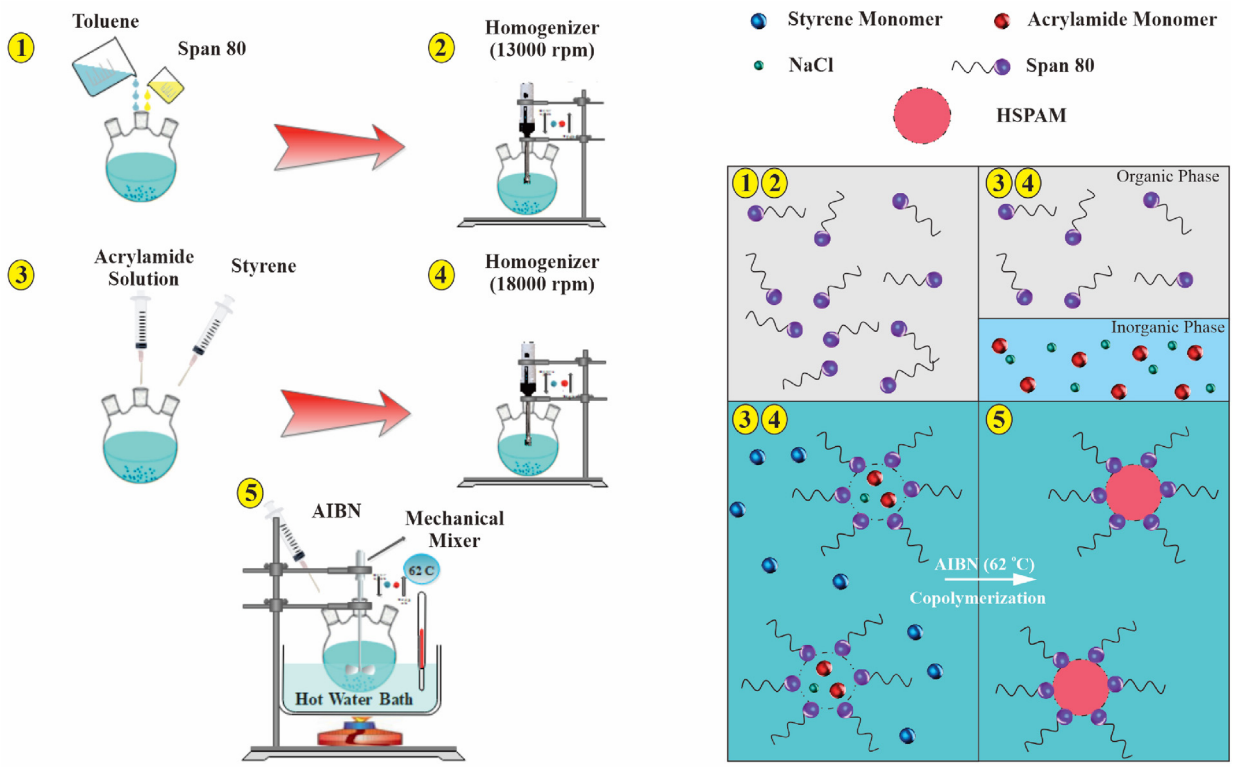

Fig. 2. Synthesis procedure schematic of styrene associating incorporated-acrylamide polymer (HSPAM).

method for the molecular weight determination and the effect of intramolecular hydrophobic interaction on the viscosity was negligible in the dilute solution [29,64].

$$\eta = kM^a \quad (3)$$

To determine the intrinsic viscosity and molecular weight of the synthesized polymer, a final emulsion portion was precipitated by an excess amount of ethanol (1:5) and washed three times by methanol, following by drying the precipitation in the oven at 50 °C for 168 h. Finally, different polymer solutions were prepared by dissolving 1.0, 1.5, 2.0, 2.5, 3.0 and 3.5 g of the white copolymer powders in 1,000 mL deionized water. The measurements in three times showed that the intrinsic viscosity and molecular weight of HSPAM polymer were 354.05 mL/g and 1×10^6 Da, respectively.

To evaluate the polymer concentration effect on the rheology behavior, polymer aqueous solutions with a desired concentration were prepared and left to be swollen well for one day; next, homogenized solutions were left again for one extra day before the analyses to eliminate air bubbles. Ubbelohde viscometer (constant factor = 0.3 mm^2/s^2) was used for determining the viscosity values versus different concentrations. Moreover, Anton Paar MCR302 rheometer was precisely applied to investigate the effect of different shear rates on the polymer solution viscosity in seawater at the ambient temperature and constant polymer concentration of 3,000 ppm.

Two different types of stability tests were carried out for the polymer solutions including polymers versus the residence time and reservoir brines [18]. The first experiment was implemented for various polymer concentrations (1000, 3000, and 5000 ppm) of HPAM and HSPAM in DIW against time at ambient temperature to check the polymers stability. For this purpose, 10 mL of polymer solutions were poured in the sealed tube tests and kept them for 120 days. The second one was conducted against seawater and formation brine with the TDS of 40,572 and 195,475 ppm at 3,000 ppm polymers concentration and 80 °C, respectively. 10 mL of HSPAM and HPAM solutions were poured in the sealed tube test and kept in an oven for 120 days [65].

2.4. Contact angle, interfacial tension, and flooding measurements

Due to the inadaptability of the glass micromodel (quartz) properties and carbonated rocks, carbonated cross-sections for WA tests and sessile drop method were used for contact angle measurements. Standard core lab procedures were also precisely implemented in the cutting, trimming, and cleaning steps of the core samples. Fig. 3 demonstrates six calcite cross sections provided for the contact angle measurement before and after the aging procedure. The cross sections were shaved and polished to reach a flat smooth surface. Next, the thin slices were washed by toluene and methanol with a Soxhlet apparatus until the colorless effluent was observed. Finally, slices were aged in the oil sample at 80 °C

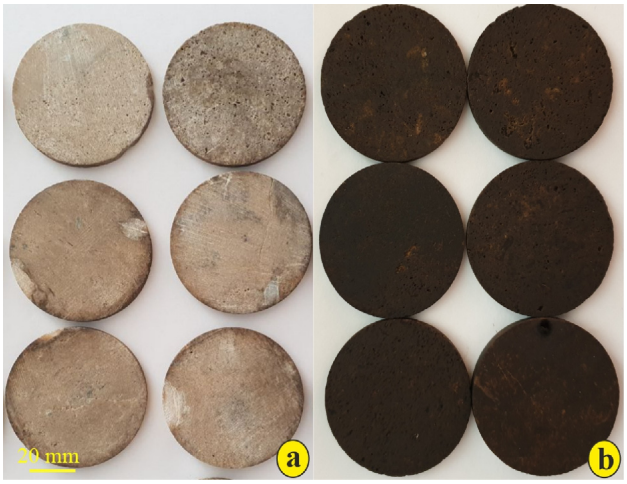

Fig. 3. Calcite cross section applied for contact angle test a) before and b) after aging with oil.

for 6 weeks to reach the oil-wet condition. The effect of different solutions was studied according to measure the net changes in the contact angle after the wettability alteration of the as-prepared slices into aqueous solutions during 72 h at the ambient condition. Contact analyses (CA) were implemented in dynamic mode by a simple and accurate setup at the ambient condition to capture the image of the drop shape by a Dino-Lite Edge digital microscope (AM-413ZT model, 200X, 1.3 mega pixel, Taiwan) [66–68]. The accuracy of the data was about ± 4%. Besides, the contact angle values were reported from the inside of the oil droplets. The effects of the different polymer solutions on the IFT value were assessed for six solutions in the absence and presence of salinity (40,572 ppm) using the pendant drop rising bubble method by VIT-6000 apparatus (Iran) at room temperature [69]. To reassure the accuracy of the results, each IFT test was performed at 4 replications.

According to Fig. 4(a), a carbonate coated glass-micromodel with dual porosity-dual permeability pattern (60 mm width, 140 mm length, 160 μm average depth, 546 mD average permeability, and 53% average porosity) was used as a porous medium in this research [62,70]. Due to the obstacle of non-repeatability results obtained from the most micromodels during flooding tests, a homogeneous double permeability pattern with a single fracture was designed to visually investigate the polymer flooding at pore scale mechanisms, dwindle the effect of injection and production pathways, increase the duration of crude-fluids-rock interaction, and decrease the uncertainties factors [62]. According to the previous researches [71–73], the presence of parallel, short length, and high number of fractures led to diminishing the final oil recovery, early breakthrough and prevent to correctly evaluate the pore scale mechanisms. In current work, the main focus was on effective mechanisms in carbonated reservoirs with lowest number of fractures, showing the presence of perpendicular fracture with the flow direction between two regions in order to assist the polymer flooding for the better sweep efficiency. As well as, the grain shapes were the same sphere in both matrix areas and the capillary pressure value was approximately kept at a constant value in each matrix. Furthermore, after each flooding test, the glass micromodel was cleaned by the toluene, acetone, distilled water, HCl acid (20% in volume), distilled water, and acetone, respectively. In the following, the micromodel was saturated with acetone and dried into an oven at 100 °C for 2 h to revert the glass micromodel into the initial wettability condition to stabilize the flooding test conditions [62]. A diluted suspension with concentration of 2 wt% $CaCO_3$ was injected to the micromodel and then dried at 80 °C for five days to obtain a homogeneous distribution in the porous media [62,74,75]. Fig. 4(b) shows the difference between a typical glass micromodel and the carbonate coated micromodel in scale of the pore structure. Before each test, the prepared micromodel was washed with toluene, deionized water and acetone, respectively [76]. Then, it was dried in the electrical laboratory oven and saturated with crude oil at least for 48 h to make it oil-wet, hence flooding experiments were carried out in the absence of initial water saturation. Under the next scenario, the chemical solution was injected into the micromodel as tertiary flooding with 0.05 mL/h (total injection time about 64 h). The laminar flow rate equaled to four pore volume (4 PV) until the oil production approximately reached zero. The recovery factor (RF) through the displacement process, pore-scale phenomena, and mechanisms were assessed by the image processing technique and Dino-Lite camera (AM-413ZT model, 200X, 1.3 mega pixel, Taiwan) [54].

3. Results and discussion

3.1. Associating copolymer characteristics

Fig. 5a, b, c show the FTIR, ^{1}H NMR, and TGA results for the prepared HSPAM and commercial PAM products, respectively. Each of the characteristic peaks in the FTIR spectra presented in Fig. 5a attributed to a specific functional group participated in the polymer structure. Table 3 gives a brief explanation of these characteristic peaks and their representative functional groups. The peaks near 3400 cm^{-1} belonged to (NH_2) group and 1700 cm^{-1} defined absorption band of (C═O) existing in polyacrylamide [29,37,77]. The range of 2800–2950 cm^{-1} and 1319 cm^{-1} related to (—CH_2—) and stretching vibration of —NH groups for both acrylamide and styrene, respectively [37,78]. The peak of 1450 cm^{-1} was owned to benzene aromatic ring in styrene. Finally, peaks in the range of 600–1300 cm^{-1} belonged to the aromatic (C—H) deformation vibrations of the aromatic ring [79]. Accordingly, HSPAM consisted of both characteristic peaks of acrylamide and styrene, revealing the presence of styrene and acrylamide monomers in the copolymer structure.

Fig. 5b demonstrates the ^{1}H NMR spectrum in which the peaks at 0.9–1.8 and 2–2.6 corresponded to aliphatic group (—CH_2—) and (—CH—) in the polymer backbone, respectively [37]. The chemical shift of the benzene ring protons as a dangling chain of styrene incorporated in the backbone appeared in 6.8–7.1, 7-3-7.7 ppm [29,37]. Characteristic peaks of acrylamide and styrene in ^{1}H NMR test proved to the existence of styrene and acrylamide units in the copolymer structure. The extra peak in the range of 3.7–4.8 ppm was due to water residual [37,63]. By ^{1}H NMR spectra in Fig. 5b and Eq. (1), (2), the styrene monomer incorporation in the hydrophilic polymer backbone was approximately 4 mol% exhibiting the associating polymer still water-soluble.

The thermal resistance of PAM and HSPAM are shown in Fig. 5c. The previous studies showed three weight loss levels depending on the different molecular weights for polyacrylamide [37,56]. There was a little weight loss of the substance (about 1%) observed below 100 °C which could be attributed to the humidity or moisture existence in inter- and intra-molecular space of HSPAM and PAM [80,81]. Showing the three degradation stages presented in Fig. 5c, the first one occurred at 141 °C where the weight loss was about 8% of the total weight for both PAM and HSPAM. The second one started at 246 °C while the weight loss was about 16% and 13% of the total weight for PAM and HSPAM, respectively. This behavior was related to the thermal parsing of the hydrophobic side chains. The third one began at about 326 °C and 341 °C alongside the weight loss of 60% and 53% of the total weight for PAM and HSPAM, respectively. This demeanor was attributed to

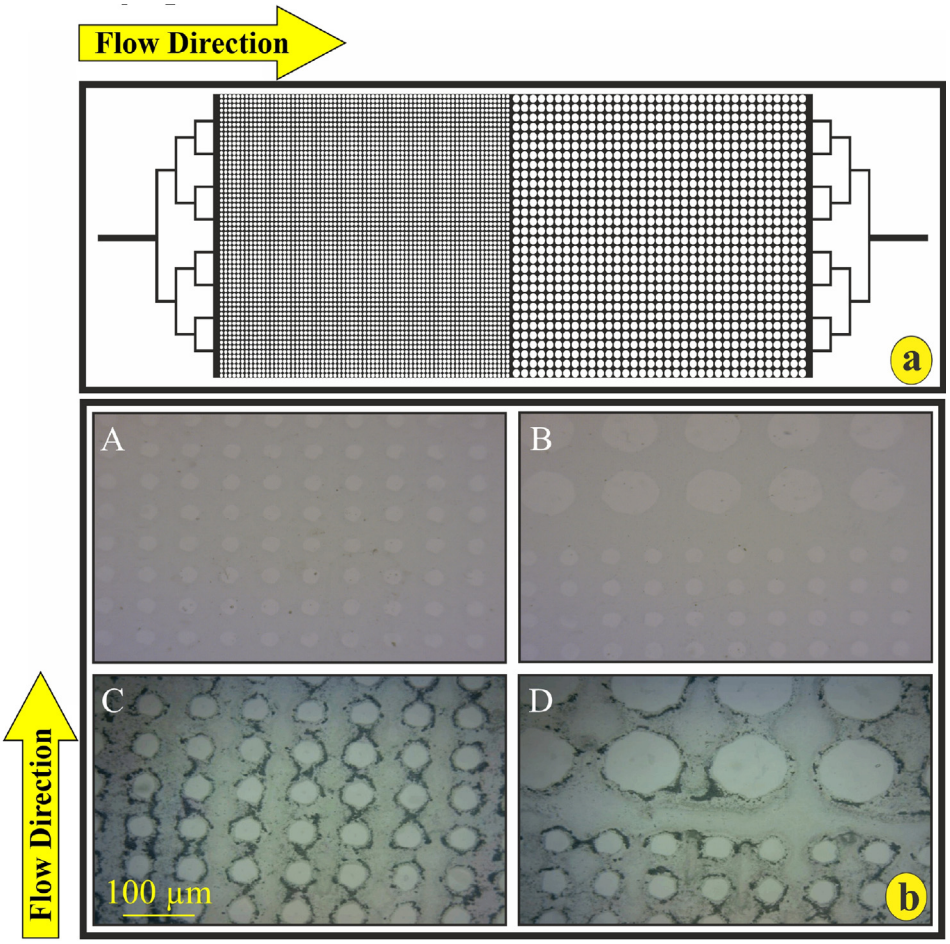

Fig. 4. a) Micromodel pattern, b) microscopic image of carbonate coated micromodel (A and B before coating, C and D after coating.

the disintegration of the amide groups as well as the polymer main chains degraded. The difference in the initial degradation temperature of these two samples was the same. However, in the second and third stage, the PAM average weight loss was higher than that of HSPAM. This behavior was due to the association of styrene chains to the acrylamide skeleton which played an important role in increasing the thermal resistance [29].

3.2. Associating polymer rheological behavior in the presence of salinity and shear rate

The critical concentration of hydrophobically associating polymers is an important factor to determine the appropriate concentration for the polymer flooding, where a drastic viscosity enhancement happened due to increase in hydrophobic bonds interactions and then resulted in the intermolecular strength [82]. The viscosity of the HSPAM and HPAM solutions versus the polymer concentration is illustrated in Fig. 6a at shear rate 0.01 s^{-1} and room temperature condition. As illustrated in Fig. 6a, the HPAM rheology behavior showed a typical intramolecular associating polymer in deionized water and a linear relation between the polymer viscosity and concentration because of the intermolecular hydrodynamic size increment [83]. Up to the first critical concentration about 2,500 ppm at which the entanglements became elastically effective. By further increasing the HSPAM concentration, the styrene hydrophobic interactions in the hydrosoluble skeleton started to self-aggregate into hydrophobic micro-domains, resulted in a sudden increment in the viscosity showing the second critical concentration of 3,000 ppm, where the intramolecular association converted to intermolecular association. The attendance of hydrophobic styrene monomers in the hydrophilic main chain caused the acquisition of unique rheological properties. Actually, this behavior was created from the intermolecular interaction in the structure of this polymer accordingly. Hydrophobic groups led to an increment in the hydrodynamic volume and finally created a positive impact on the aqueous solution macroscopic viscosity enhancement. At lower concentrations before the first critical value, the viscosity enhancement behavior was linear for both polymeric samples, however, the dynamic viscosity for HPAM was more than that of HSPAM. This behavior was due to overcoming higher molecular weight of HPAM in rather than the microscopically hydrophobic associating in HSPAM in attempt to participate in the viscosity enhancement process that was inversely happened by further increasing the concentration intersected at 3,500 ppm [18,29,41]. The results from Fig. 6b showed that the viscosity of both solutions was reduced after increasing the shear rate. Albeit, the viscosity reduction slope in the HSPAM solution was lower than that of HPAM, probably because of the existence of the styrene associations in the polymer chains improved the resistance of HSPAM against the high shear rates [40,84]. Fig. 6c shows the changes of the dynamic viscosity of the HSPAM and HPAM aqueous solution (C_p = 3,000 ppm) in the absence and presence of salinity (40,572 ppm) at shear rate 0.01 s^{-1} and room temperature. The viscosity of HPAM and HSPAM in deionized water were found to be 142.3 and 121.2 mPa.s, respectively. On the other side, the presence of salinity in seawater dwindled the viscosity of HPAM + SW solution, while the viscosity of the HSPAM + SW solution increased up to 147.3 mPa.s. Unlikely,

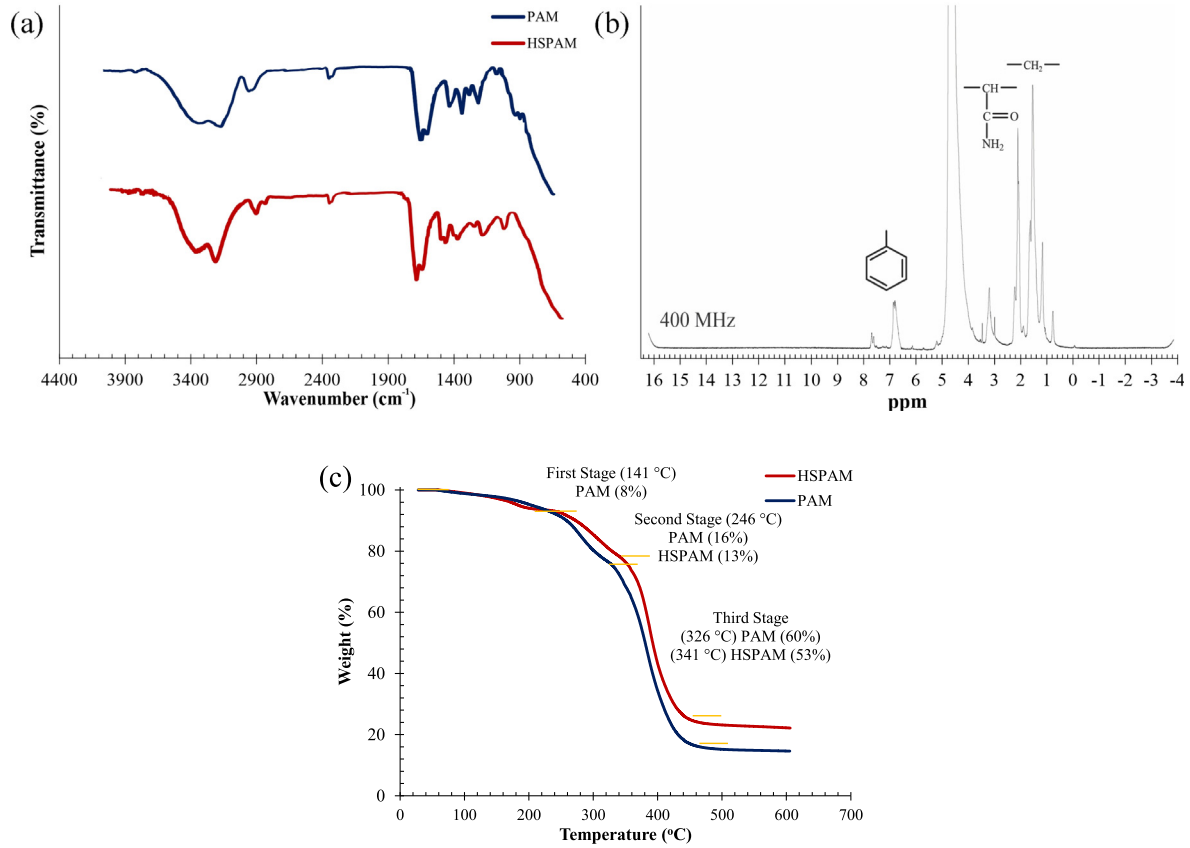

Fig. 5. (a) FTIR spectra, (b) ^{1}H NMR spectra, and (c) thermogravimetric analysis curves for HSPAM and PAM samples.

Table 3
Characteristic peaks of PAM and HSPAM in FTIR spectra.

Peaks (cm^{-1})	PAM	HSPAM
C—H deformation vibrations of aromatic ring	–	~ 930
Stretching vibration of —NH groups	1319	1319
Benzene aromatic C—C band stretch	–	1450
C—N stretching group in AM	1450 & 1615	1450 & 1615
Absorption band of C=O in AM	1675	1675
CH_2 group	2926	2926
NH_2 group in AM	3400	3400

the viscosity of the HPAM + SW solution significantly dropped at the high salinity condition due to the important electrostatic repulsion among the polymer chains to prevent the typical intramolecular associating. Refer to schematically presented in Fig. 6d, in the case of HSPAM + SW solution, the existence of the divalent and monovalent cations in the aqueous solution helped to the more intermolecular associations resulted from the salting out phenomenon and decreasing repulsion of the charged partial hydrolysis of the amide groups [40,85–87]. This phenomenon confirmed the ability of this simple hydrophobically associating polymer to have the better performance under harsh reservoir conditions compared to conventional HPAM.

Fig. 7 shows the polymer stability test versus time and different salinities after 120 days. The polymer compatibility with the reservoir brines was conducted to investigate the adaptability of cation and anion ions with polymers in the saline aqueous solutions to avoid the undesirable polymer precipitation during the flooding process. Results from Fig. 7a and b demonstrated the HSPAM and HPAM samples prepared by different polymer concentrations had a great stability after 120 days at the room temperature and zero salt content confirmed the polymer synthesis quality. The polymer stability against the saline water at high temperature of 80 °C is illustrated in Fig. 6c and d. No precipitation was occurred for HSPAM dissolved in different salinities (40,572 and 195,475 ppm) after 120 days. In the event that HPAM was considerably participated in the both saline waters and the precipitates in FB were higher compared to SW due to the higher amount of divalent and monovalent ions concentration.

3.3. EOR application study of associating polymer

This section provided results of the rock/fluid and fluid/fluid interaction combining with micromodel flooding experiments in the absence and presence of the salinity to evaluate the HSPAM solution behavior through the enhanced oil recovery process compared to HPAM.

WA test was performed on six solutions containing HSPAM and HPAM (C_p = 3,000 ppm) to check the chemical composition effect on the rock surface. The net value differences for the calcite wettability alteration by SW, DIW, and HSPAM and HPAM in DIW and SW solutions are demonstrated in Fig. 8a and b at room temperature. Despite all the cross sections became strongly oil-wet, the initial contact angle was not the same for the rock slices, it was probably attributed to the rock surface heterogeneity [69]. Table 4 represents the net change of WA after 72 h between aqueous solutions, crude oil droplet, and calcite cross sections. The anionic HPAM changed the surface wettability better than HSPAM in deionized water after 72 h which was a great impact on calcite rock slices and able to desorb the oil droplet from the rock surfaces. Polyacrylamide in the HPAM sample was partially hydrolyzed to replace the amide groups (–$CONH_2$) by carboxyl groups (—COO—) which created negative charges, strongly affecting the polymer adsorption on surface slices after 72 h. The lack of divalent ions

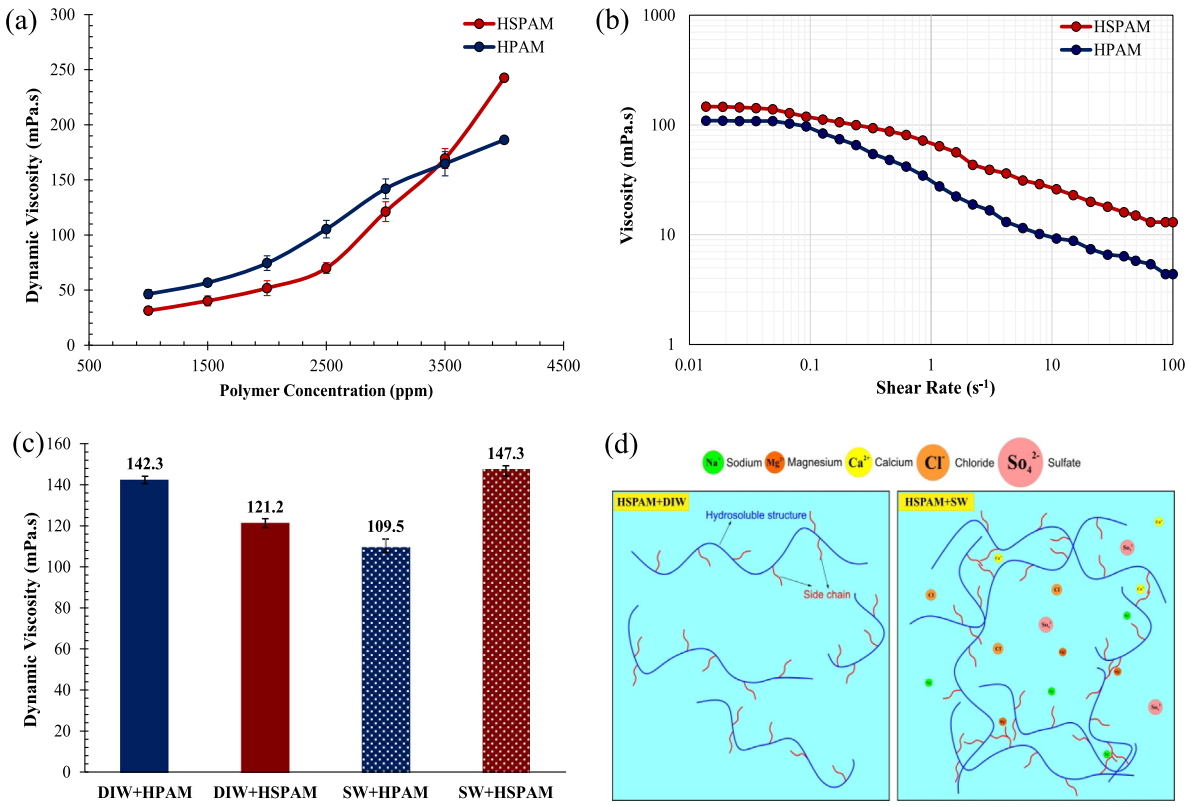

Fig. 6. Dynamic viscosity of HSPAM and HPAM aqueous solution (a) at different polymer concentrations, 0.01 s^{-1} shear rate, room temperature, zero TDS, (b) at different shear rates in synthetic seawater at room temperature, C_p = 3,000 ppm, (c) at different salinity concentrations, 0.01 s^{-1} shear rate, room temperature, C_p = 3,000 ppm, (d) viscosity enhancement mechanism by HSPAM + DIW and HSPAM + SW.

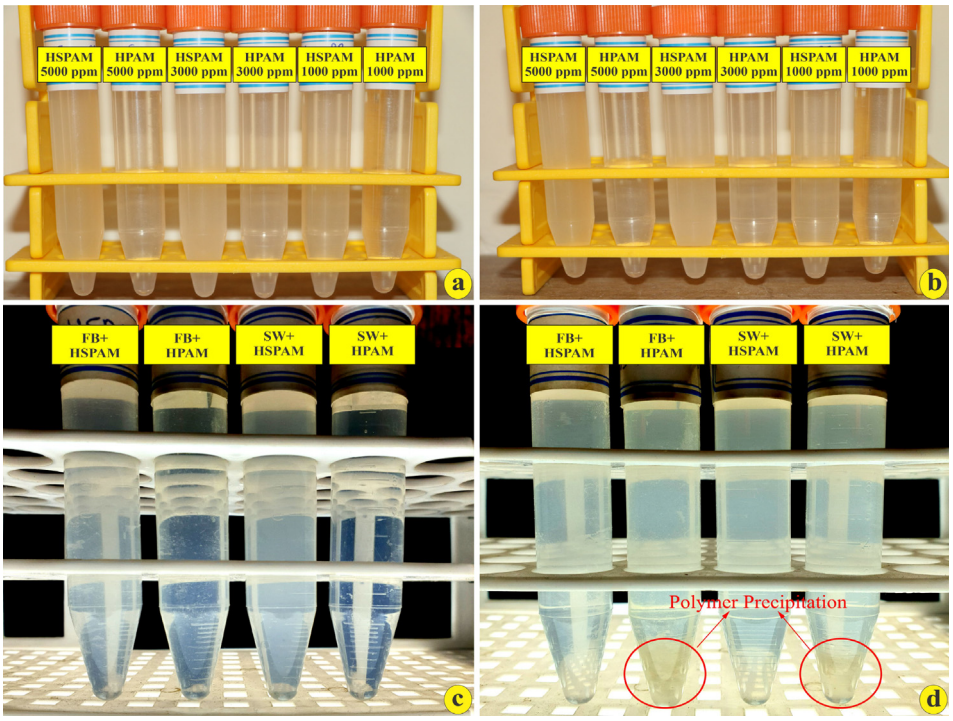

Fig. 7. Stability test versus time for different polymer concertation in DIW: a) initial condition and b) after 120 days in ambient condition, stability test for polymer concertation of 3,000 ppm versus different salinities of SW and FB: c) initial condition and d) after 120 days at high temperature of 80 °C.

in deionized water provided a neutral environment for the intermolecular association of the synthesized polymer to not be activated in the wettability alteration process. Hence, the CA value for HSPAM was lower compared to that of HPAM due to the hydrophobic bonds that were still inactive in the absence of salinity. On the other side, the effect of HSPAM on the WA value was

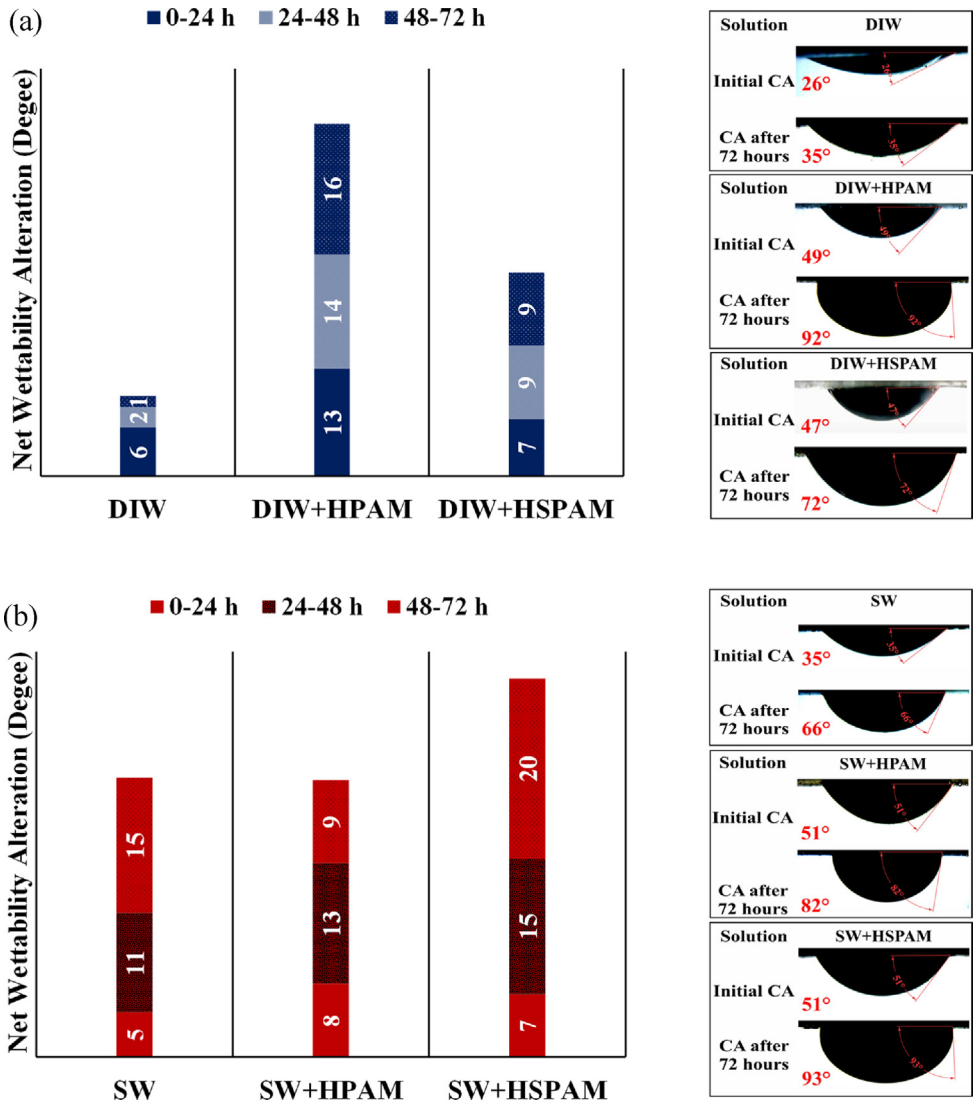

Fig. 8. Oil contact angle measurements by HPAM and HSPAM at (a) deionized water and (b) seawater, C_p = 3,000 ppm and room temperature.

Table 4
Net change of calcite wettability alteration by aqueous solutions after 72 h.

Solution type	DIW	SW	DIW + HPAM	DIW + HSPAM	SW + HPAM	SW + HSPAM
CA alteration after 72 h	9°	31°	43°	25°	31°	42°

better than HPAM dissolved in seawater. The activity of hydrophobic bonds increased in the presence of divalent cations (Ca^{2+} and Mg^{2+}) in seawater which led to desorb the carboxylic groups from the rock surfaces in order to improve the wettability alteration. As well as, the presence of free calcium and magnesium and also sulfate active ions into the aqueous solution assisted HSPAM to desorb the crude oil from the rock in attempt to increase the synergistic effect of HSPAM + SW in changing the rock wettability from oil-wet to more water-wet state [62,88–90]. Moreover, the existence of the styrene monomer in HSPAM as an oil derivative played a key role in the better interaction between the oil and polymer. Whereas, the surface wettability alteration value was decreased by HPAM + SW solution compared to HPAM + DIW, this behavior resulted from the HPAM chain agglomeration in the presence of monovalent and divalent cations during the WA process. Because of this interaction, a large number of cations also became out of service to participate in the wettability modification procedure. These results revealed that the novel hydrophobically association polymer was capable to improve the wettability modification of the calcite rock from a strongly oil-wet to a mixed-wet even at high salinity reservoir conditions.

IFT measurement was done to investigate about the impact of HSPAM and HPAM solutions (Cp = 3,000 ppm) on the fluid/fluid interaction in the both absence and presence of salinity. As presented in Fig. 9, the IFT results were approximately the same for all samples. The main mechanism underlying the IFT reduction for seawater could be the tendency of cations and anions for migrating to the oil–water interface and had an effective chemical interaction with natural surface-active agent from crude oil (resin and asphaltene) [91–95]. Making solutions by HSPAM in DIW and SW resulted in a little higher IFT reduction (16% and 12%, respectively), due to completely activating the hydrophobic chains by

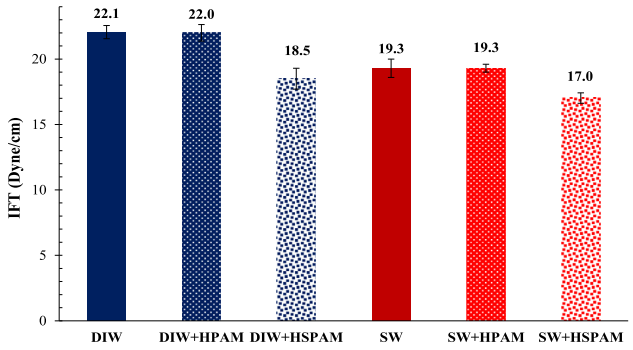

Fig. 9. IFT measurements for polymer solutions in dionized water and seawater at C_p = 3,000 ppm and room temperature.

the existence of monovalent and divalent cations in SW. Besides, the existence of hydrophobic styrene chains as an oil derivative material provided a better interaction among crude oil components compared to the HPAM solution to assist the higher IFT reduction. These tests revealed that the presence of hydrophobic bonds in the chemical structure of the associative polymer could promote the interactions between the water and oil interface and possibly work as a weak low surface energy agent.

After analyzing the polymer behaviors on the rock/fluid and fluid/fluid interactions affected by the salinity value, carbonate coated micromodel flooding tests were implemented by six different solutions to show the results of the recovery factors. Figs. 10 and 11 demonstrate a comparative ultimate oil recovery after the four-pore volume injection for the continuous polymer flooding after the water and brine flooding. The amount of recovery factor for DIW + HPAM, SW + HSPAM, DIW + HSPAM, and SW + HPAM was 78.2, 82.0, 65.0, and 61.2 OOIP%, respectively. Furthermore, DIW and SW recovery factors for the secondary flooding process were 26.2 and 30.4 in the case of HSPAM and 25.3 and 31.4 OOIP % in the case of HPAM, respectively. Final polymer flooding results were obtained due to the viscosity enhancement and CA alteration as a strongly recovery mechanisms and IFT reduction as a weakly recovery mechanism discussed in the previous parts as the below sequences, respectively:

Viscosity enhancement: SW + HSPAM > DIW + HPAM > DIW + HSPAM > SW + HPAM

Wettability modification: DIW + HPAM ~ SW + HSPAM > SW + HPAM > DIW + HSPAM > SW > DIW

IFT Reduction: DIW ~ DIW + HPAM < SW ~ SW + HPAM < DIW + HSPAM < SW + HSPAM

Based on the rheology and wettability alteration results, the viscosity values for SW + HSPAM and DIW + HPAM were almost equal and both solutions had the same contact angle. Although, SW + HSPAM solution reduced the IFT by 5.1 dyne/cm more than that of DIW + HPAM due to the activated of hydrophobic styrene chains with divalent cations of SW. Therefore, according to Eq. (4), capillary force was decreased by IFT reduction (δ) at constant contact angle (cosθ) and pore radius (r). Furthermore, Eq. (5) illustrates capillary number increased by decreasing the capillary force while the viscous force was constant.

$$\text{Capillary Forces} = \frac{2\sigma\cos\theta}{r} \tag{4}$$

$$\text{Capillary Number} = \frac{\text{Viscous Force}}{\text{Capillary Force}} \tag{5}$$

All in all, when two different polymer solutions had approximately the same viscosity and contact angle, the one created the less IFT had a higher capillary number. As well as, the capillary number had a direct relationship with the sweep efficiency and recovery factor performance. Hence, the sweep efficiency of SW + HSPAM was more than DIW + HPAM due to the higher capillary number. This phenomenon was clearly showed in the SW + HSPAM and DIW + HPAM sections of Fig. 11, especially in the low permeability side of the carbonate coated micromodel.

The performance of HPAM in DIW was better than in saline environments (SW), confirming the HPAM degradation under the harsh saline environments. On the contrary, the potential of HSPAM in the oil recovery improvement increased by the salinity increment, in a way that SW + HSPAM solution yielded the maximum recovery of OOIP compared to SW + HPAM.

3.4. Microscopic emulsification and coalition mechanisms of oil recovery

According to Eq. (6), colloidal instability index (CII) expresses the sum of saturates and asphaltenes per the sum of aromatics and resins. CII of crude oil higher than 0.9 implies the unstable asphaltene on the edge of precipitation [96]. Moreover, asphaltene plays a key role on the water production in oil (W/O) emulsions [97]. CII of the crude oil used in this study was approximately 1.18 which was a great potential for the emulsification process during the water flooding.

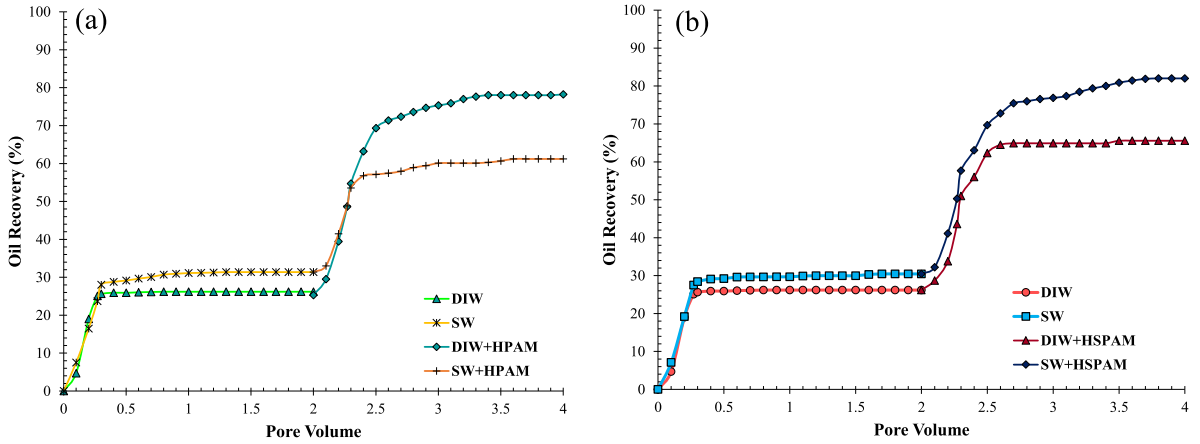

Fig. 10. Oil recovery factor of DIW and SW secondary and tertiary flooding in the presence and absence of a) HPAM and b) HSPAM, C_p = 3,000 ppm, 4 PV injection, room temperature, 64 h.

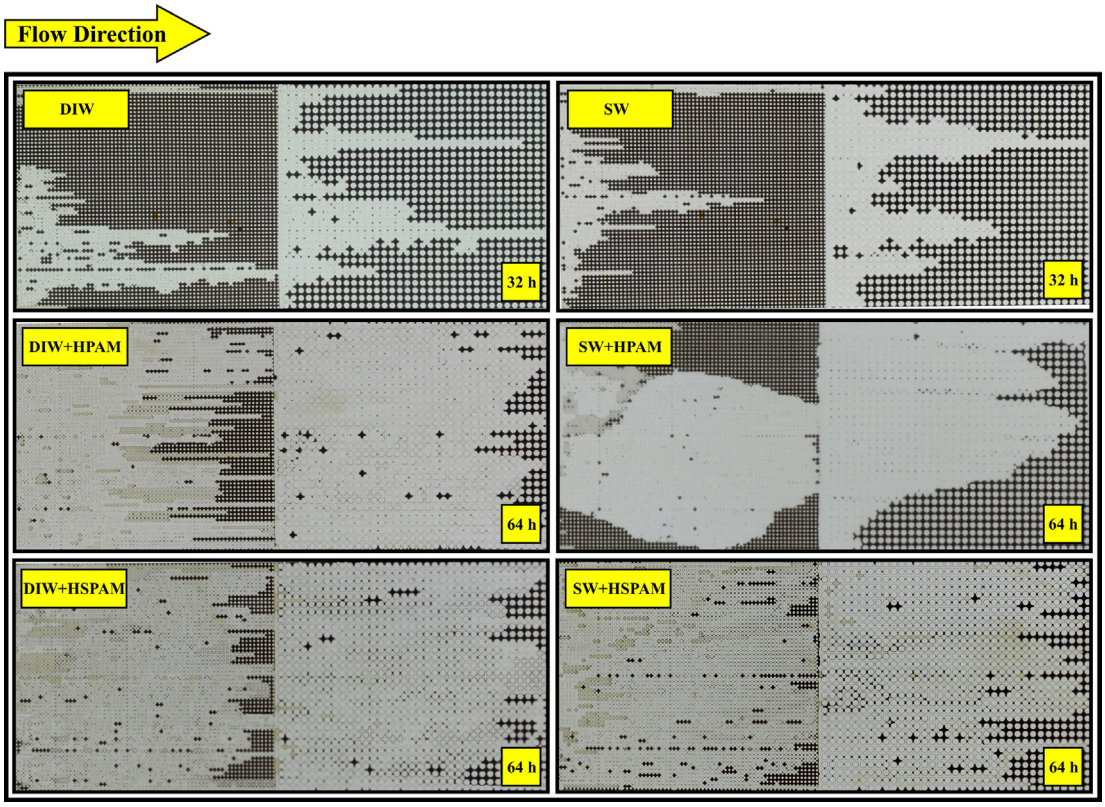

Fig. 11. Snapshots of DIW and SW secondary and tertiary flooding in the presence and absence of HPAM and HSPAM, C_p = 3,000 ppm, 4 PV injection, room temperature, 64 h.

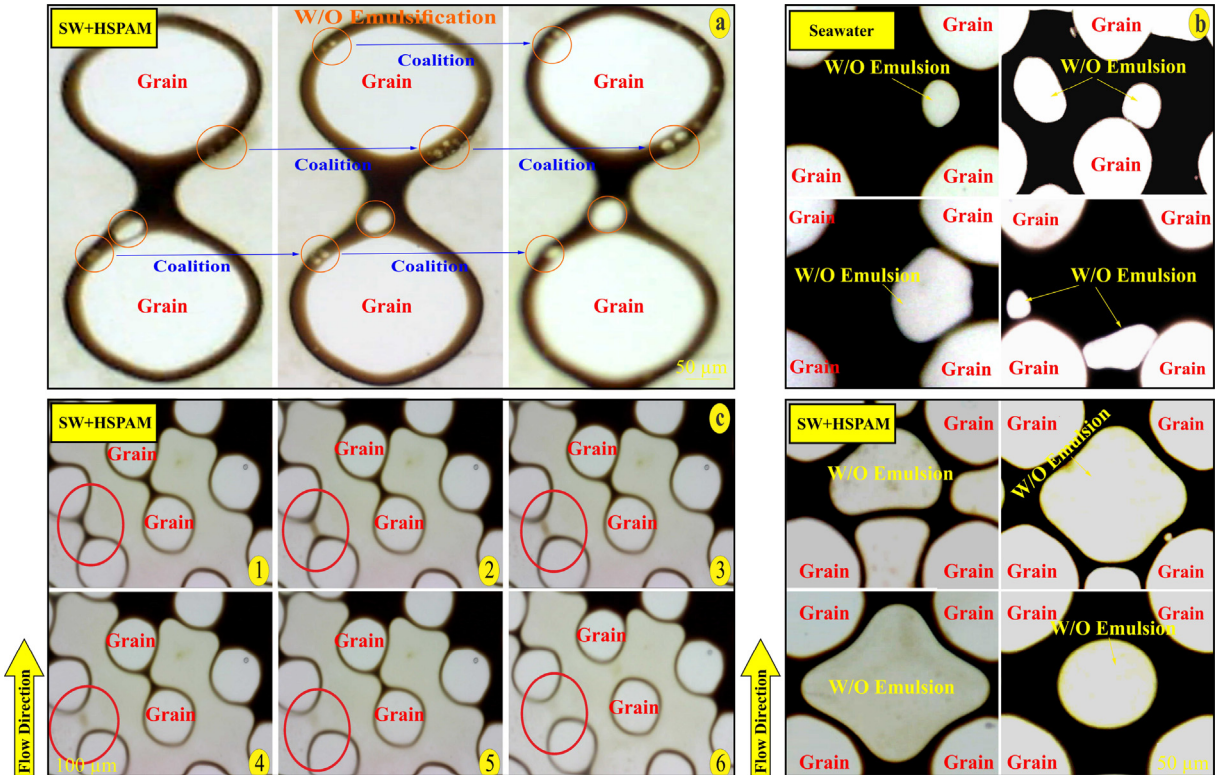

Fig. 12. a) Effect of HSPAM on W/O emulsification and coalition process, b) evidence of water in oil emulsification, c) mass transfer effect during HSPAM flooding after 4 PV injection in carbonate coated glass micromodel (all tests at room temperature, W/O emulsification process and coalition indicated by orange circles and blue arrows).

$$CII = \frac{Saturates + Aspaltenes}{Aromatics + Resins} \quad (6)$$

The presence of surface-active materials like Mg^{2+}, Ca^{2+}, resin, and asphaltene as the third components through the emulsification process resulted in the IFT reduction between oil/water phases, stabilized and increased the number of dispersed droplets [76]. As mentioned before, the presence of divalent cations activated the hydrophobic styrene dangling chains of HSPAM to effectively IFT reduction. Thus, SW and SW + HSPAM solutions showed a higher potential for the emulsification.

Fig. 12a illustrates the existence of W/O emulsions in the separated oil layer in the case of the SW + HSPAM flooding process. Through the flooding, the volume of oil layer increased due to coalition of W/O emulsions leading to finally intensify the swelling of oil layer. This phenomenon continued until the trapped oil was moved and produced [72,76]. Fig. 12b shows the water trapping happened among the pores in the oil phase for the SW and SW + HSPAM solutions. The results revealed that trapped water droplets in the SW + HSPAM solution were much bigger than droplets of SW that completely filled the pores and pore throats in some areas. These trapped water phase pushed the oil phase by its higher viscosity frontier from the middle of pore structures to the production outlet leading to improve the recovery factor. On the other side, the velocity of the oil phase flow increased by decreasing the radius of pore throats. Pores filled with the water phase did not permit the behind oil phase to stow the pores and reserve due to the higher viscosity of HSPAM included in the water phase than that of the oil phase. This mechanism could also change the injection flow from high permeable to uninvaded low permeable sections to enhance the sweep efficiency and oil recovery by minimizing the viscous fingering. Fig. 12c shows a microscopic mechanism that could be probably due to the mass transfer between the water and oil phases by reducing the IFT with active styrene chain in the presence of divalent cations.

4. Conclusions

This study outlined the rheology, wettability alteration, and flooding characteristics of a new hydrophobically associating copolymer synthesized by styrene and acrylamide at the high temperature and high salinity condition by checking three main oil recovery mechanisms. It was polymerized by acrylamide (a hydrosoluble monomer to viscosify the water pushing phase) and styrene (available, simple, and oil derivative monomer to viscosifying associations, alter the fluid-rock wettability, and reduce fluid-fluid IFT) through inverse emulsion polymerization method. The most essential findings were summarized below:

- Implementing characterization tests showed the presence of hydrophobic styrene and hydrophilic acrylamide monomers in the polymer chain. Besides, TGA result revealed an appropriate thermal stability for the produced copolymer considered at high temperature reservoir.
- Rheology tests conducted in deionized water and in the presence of 40,572 ppm salinity suggested that unlike the common polymers such as HPAM which lost their viscosifying property in the presence of monovalent and divalent cations, HSPAM not only was resistant to these ions, but also a significant increase was observed in the solution viscosity with the salinity increment. Besides, the slope of viscosity reduction for the HSPAM aqueous solution versus the shear rate was lower compared to HPAM in the presence of salinity.
- Both HSPAM and HPAM showed a great stability without any precipitation against time in DIW after 120 days at the ambient temperature. Also, HSPAM was completely stable in different salinities compared to HPAM after 120 days at 80 °C.
- Addition of HSPAM in seawater led to a more water-wet state after 72 h and a better IFT reduction compared to HPAM presenting the below sequences for the wettability modification and IFT results:
  DIW + HPAM ~ SW + HSPAM > SW + HPAM > DIW + HSPAM > SW > DIW
  DIW ~ DIW + HPAM < SW ~ SW + HPAM < DIW + HSPAM < SW + HSPAM
- The micromodel flooding results also revealed the most oil recovery was attributed to SW + HSPAM about 82 OOIP%. Besides, microscopic snapshot revealed that the synergistic effect of SW + HSPAM had a better performance in the W/O emulsification process among grains and pore throats to have a great impact on producing the residual oil after the breakthrough. The oil recovery factors were obtained by the below sequences:
  DIW + HPAM ~ SW + HSPAM > DIW + HSPAM > SW + HPAM > SW > DIW.

CRediT authorship contribution statement

A. Maghsoudian: Formal analysis, Data curation, Writing - original draft, Conceptualization. **Y. Tamsilian:** Conceptualization, Methodology, Supervision, Writing - review & editing. **S. Kord:** Conceptualization, Methodology, Supervision, Writing - review & editing. **B. Soltani Soulgani:** Writing - review & editing. **A. Esfandiarian:** Data curation, Investigation. **M. Shajirat:** Investigation.

Declaration of Competing Interest

The authors declare that they have no known competing financial interests or personal relationships that could have appeared to influence the work reported in this paper.

References

[1] A.N. El-hoshoudy, E.M. Mansour, S.M. Desouky, Experimental, computational and simulation oversight of silica-co-poly acrylates composite prepared by surfactant-stabilized emulsion for polymer flooding in unconsolidated sandstone reservoirs, J. Mol. Liq. 308 (2020) 113082.
[2] P. Mehrabianfar, H. Bahraminejad, A.K. Manshad, An introductory investigation of a polymeric surfactant from a new natural source in chemical enhanced oil recovery (CEOR), J. Petrol. Sci. Eng. 198 (2021) 108172.
[3] Y. Zhou, X. Wu, X. Zhong, S. Reagen, S. Zhang, W. Sun, et al., Polymer nanoparticles based nano-fluid for enhanced oil recovery at harsh formation conditions, Fuel 267 (2020) 117251.
[4] A.K. Alhuraishawy, B. Bai, A. Imqam, M. Wei, Experimental study of combining low salinity water flooding and preformed particle gel to enhance oil recovery for fractured carbonate reservoirs, Fuel 214 (2018) 342–350.
[5] F. Pan, Z. Zhang, X. Zhang, A. Davarpanah, Impact of anionic and cationic surfactants interfacial tension on the oil recovery enhancement, Powder Technol. 373 (2020) 93–98.
[6] N. Li, X.-N. Bao, Y.-J. Guo, S.-Z. Yang, Y.-C. Li, B.-Z. Mu, A novel binary flooding system of a biobased surfactant and hydrophobically associating polymer with ultralow interfacial tensions, RSC Adv. 8 (41) (2018) 22986–22990.
[7] L. Buryakovsky, G. Chilingar, H.H. Rieke, S. Shin, Fundamentals of the Petrophysics of Oil and Gas Reservoirs, John Wiley & Sons, 2012.
[8] A. Esfandiarian, A. Maghsoudian, M. Shirazi, M. Mohammadi, S. Kord, Y. Tamsilian, Experimental investigation of using ionic-liquids as alternatives of surfactants in enhanced-oil-recovery processes for harsh carbonate reservoirs, in: 82nd EAGE Annual Conference & Exhibition. 2020, European Association of Geoscientists & Engineers, 2020, 1–5.
[9] M. Ding, Y. Wang, F. Yuan, H. Zhao, Z. Li, A comparative study of the mechanism and performance of surfactant-and alkali-polymer flooding in heavy-oil recovery 115603 Chem. Eng. Sci. (2020).
[10] E. Manrique, M. Ahmadi, S. Samani, Historical and recent observations in polymer floods: an update review, CT&F-Ciencia, Tecnología y Futuro 6 (5) (2017) 17–48.

[11] S.K. Veerabhadrappa, A. Doda, J.J. Trivedi, E. Kuru, On the effect of polymer elasticity on secondary and tertiary oil recovery, Ind. Eng. Chem. Res. 52 (51) (2013) 18421–18428.
[12] M. Duan, Z. He, X. Wang, B. Jing, Z. Xu, Y. Xiong, et al., A novel interface-active cationic flocculant for the oil-water separation of oily wastewater produced from polymer flooding, J. Mol. Liq. 286 (2019) 110868.
[13] R. Elhaei, R. Kharrat, M. Madani, Stability, flocculation, and rheological behavior of silica suspension-augmented polyacrylamide and the possibility to improve polymer flooding functionality 114572 J. Mol. Liq. (2020).
[14] J.J. Sheng, B. Leonhardt, N. Azri, Status of polymer-flooding technology, J. Can. Pet. Technol. 54 (02) (2015) 116–126.
[15] H. Saboorian-Jooybari, M. Dejam, Z. Chen, Heavy oil polymer flooding from laboratory core floods to pilot tests and field applications: Half-century studies, J. Petrol. Sci. Eng. 142 (2016) 85–100.
[16] A. Maghsoudian, A. Esfandiarian, A. Izadpanahi, M. Hasanzadeh, F. Famoori, Applying the synergistic effect of chemically low salinity water flooding assisted fines migration in coated micromodel, in: 82nd EAGE Annual Conference & Exhibition. 2020, European Association of Geoscientists & Engineers, 2020, 1–5.
[17] A. Zhang, Z. Fan, L. Zhao, C. He, An investigation on sensitivity analysis and performance prediction of profile control by clay particles for polymer flooded reservoir, J. Petrol. Sci. Eng. 196 (2021) 107690.
[18] M.S. Kamal, A.S. Sultan, U.A. Al-Mubaiyedh, I.A. Hussein, Review on polymer flooding: rheology, adsorption, stability, and field applications of various polymer systems, Polym. Rev. 55 (3) (2015) 491–530.
[19] K. Liang, P. Han, Q. Chen, X. Su, Y. Feng, Comparative study on enhancing oil recovery under high temperature and high salinity: polysaccharides versus synthetic polymer, ACS Omega 4 (6) (2019) 10620–10628.
[20] Y. Tamsilian, M. Shirazi, J.J. Sheng, A. Agirre, M. Fernandez, R. Tomovska, Advanced oil recovery by high molar mass thermoassociating graft copolymers, J. Petrol. Sci. Eng. 192 (2020) 107290.
[21] X. Shang, Y. Bai, K. Lv, C. Dong, Experimental study on viscosity and flow characteristics of a clay-intercalated polymer, J. Mol. Liq. 322 (2021) 114931.
[22] E. Unsal, A. Ten Berge, D. Wever, Low salinity polymer flooding: Lower polymer retention and improved injectivity, J. Petrol. Sci. Eng. 163 (2018) 671–682.
[23] Y. Lee, W. Lee, Y. Jang, W. Sung, Oil recovery by low-salinity polymer flooding in carbonate oil reservoirs, J. Petrol. Sci. Eng. 181 (2019) 106211.
[24] M. Han, A. AlSofi, A. Fuseni, X. Zhou, S. Hassan, Development of chemical EOR formulations for a high temperature and high salinity carbonate reservoir, in: IPTC 2013: International Petroleum Technology Conference, European Association of Geoscientists & Engineers, 2013, cp-350-00486.
[25] P. Ghosh, K.K. Mohanty, Study of surfactant-polymer flooding in high-temperature and high-salinity carbonate rocks, Energy Fuels 33 (5) (2019) 4130–4145.
[26] Xu.Z. Li Xe, H. Yin, Y. Feng, H. Quan, Comparative studies on enhanced oil recovery: Thermoviscosifying polymer versus polyacrylamide, Energy Fuels 31 (3) (2017) 2479–2487.
[27] B. Wei, L. Romero-Zerón, D. Rodrigue, Evaluation of two new self-assembly polymeric systems for enhanced heavy oil recovery, Ind. Eng. Chem. Res. 53 (43) (2014) 16600–16611.
[28] T. Ahsani, Y. Tamsilian, A. Rezaei, Molecular dynamic simulation and experimental study of wettability alteration by hydrolyzed polyacrylamide for enhanced oil recovery: A new finding for polymer flooding process, J. Petrol. Sci. Eng. 196 (2021) 108029.
[29] Z. Lalehgani, S.A.A. Ramazani, Y. Tamsilian, M. Shirazi, Inverse emulsion polymerization of triple monomers of acrylamide, maleic anhydride, and styrene to achieve highly hydrophilic–hydrophobic modified polyacrylamide, J. Appl. Polym. Sci. 136 (29) (2019) 47753.
[30] A. El-Hoshoudy, S. Desouky, A. Al-Sabagh, M. Betiha, M.Y. E-k, S. Mahmoud, Evaluation of solution and rheological properties for hydrophobically associated polyacrylamide copolymer as a promised enhanced oil recovery candidate, Egypt. J. Pet. 26 (3) (2017) 779–785.
[31] W. Zhou, J. Zhang, M. Han, W. Xiang, G. Feng, W. Jiang, Application of hydrophobically associating water-soluble polymer for polymer flooding in China offshore heavy oilfield, in: International Petroleum Technology Conference, International Petroleum Technology Conference, 2007.
[32] C. Zhang, P. Wang, G. Song, Performance evaluation of STARPAM polymer and application in high temperature and salinity reservoir, Int. J. Anal. Chem. 2018 (2018), 9653953.
[33] L. Qingxiang, N. Patiguli, X. Xiangxing, L. Ronghua, A comprehensive comparative appraisal of standard HPAM polymer and salt tolerant polymer KYPAM for EOR, Oilfield Chem. 24 (2) (2007) 146–149.
[34] K.G. Uranta, S.R. Gomari, P. Russell, F. Hamad, Application of polymer integration technique for enhancing polyacrylamide (PAM) performance in high temperature and high salinity reservoirs, Heliyon 5 (7) (2019) e02113.
[35] M.M. Abdullah, A.A. AlQuraishi, H.A. Allohedan, A.O. AlMansour, A.M. Atta, Synthesis of novel water soluble poly (ionic liquids) based on quaternary ammonium acrylamidomethyl propane sulfonate for enhanced oil recovery, J. Mol. Liq. 233 (2017) 508–516.
[36] J.T. Ma, R.H. Huang, L. Zhao, X. Zhang, Solution properties of ionic hydrophobically associating polyacrylamide with an arylalkyl group, J. Appl. Polym. Sci. 97 (1) (2005) 316–321.
[37] M. Shaban, A.R. SA, M. Ahadian, Y. Tamsilian, A. Weber, Facile synthesis of cauliflower-like hydrophobically modified polyacrylamide nanospheres by aerosol-photopolymerization, Eur. Polym. J. 83 (2016) 323–336.
[38] M.R. Aguilar, J. San Román, Introduction to Smart Polymers and their Applications. Smart Polymers and their Applications, Elsevier, 2019, p. 1–11.
[39] H. Yang, H. Zhang, W. Zheng, B. Zhou, H. Zhao, X. Li, et al., Effect of hydrophobic group content on the properties of betaine-type binary amphiphilic polymer, J. Mol. Liq. 311 (2020) 113358.
[40] D. Wever, F. Picchioni, A. Broekhuis, Polymers for enhanced oil recovery: a paradigm for structure–property relationship in aqueous solution, Prog. Polym. Sci. 36 (11) (2011) 1558–1628.
[41] K.C. Taylor, H.A. Nasr-El-Din, Hydrophobically Associating Polymers for Oil Field Applications, Canadian International Petroleum Conference, All Days, 2007.
[42] K.C. Taylor, H.A. Nasr-El-Din, Water-soluble hydrophobically associating polymers for improved oil recovery: A literature review, J. Petrol. Sci. Eng. 19 (3–4) (1998) 265–280.
[43] R.O. Afolabi, G.F. Oluyemi, S. Officer, J.O. Ugwu, Hydrophobically associating polymers for enhanced oil recovery – Part A: A review on the effects of some key reservoir conditions, J. Petrol. Sci. Eng. 180 (2019) 681–698.
[44] L. Jian-xin, G. Yong-jun, H. Jun, Z. Jian, L. Xing, Z. Xin-ming, et al., Displacement characters of combination flooding systems consisting of gemini-nonionic mixed surfactant and hydrophobically associating polyacrylamide for bohai offshoreoilfield, Energy Fuels 26 (5) (2012) 2858–2864.
[45] A. El Hoshoudy, S. Desouky, A. Al-sabagh, M. El-kady, M. Betiha, S. Mahmoud, Synthesis and characterization of polyacrylamide crosslinked copolymer for enhanced oil recovery and rock wettability alteration, Int. J. Oil, Gas Coal Eng. 3 (4) (2015) 43–55.
[46] T. Shen, H. Zhou, X. Liu, Y. Fan, D.D. Mishra, Q. Fan, et al., Wettability control of interfaces for high-performance organic thin-film transistors by soluble insulating polymer films, ACS Omega 5 (19) (2020) 10891–10899.
[47] A. Al-Sabagh, N. Kandile, R. El-Ghazawy, M.N. El-Din, E. El-Sharaky, Solution properties of hydrophobically modified polyacrylamides and their potential use for polymer flooding application, Egypt. J. Pet. 25 (4) (2016) 433–444.
[48] M. Pancharoen, M.R. Thiele, A.R. Kovscek, Inaccessible pore volume of associative polymer floods, in: SPE Improved Oil Recovery Symposium, Society of Petroleum Engineers, 2010.
[49] K. Xie, X. Lu, Q. Li, W. Jiang, Q. Yu, Analysis of reservoir applicability of hydrophobically associating polymer, SPE J. 21 (01) (2016) 1–9.
[50] F.R. Wassmuth, K. Green, J. Bai, Associative polymers outperform regular polymers displacing heavy oil in heterogeneous systems, in: SPE Heavy Oil Conference Canada, Society of Petroleum Engineers, 2012.
[51] L. Petit, C. Karakasyan, N. Pantoustier, D. Hourdet, Synthesis of graft polyacrylamide with responsive self-assembling properties in aqueous media, Polymer 48 (24) (2007) 7098–7112.
[52] P. Raffa, A.A. Broekhuis, F. Picchioni, Polymeric surfactants for enhanced oil recovery: A review, J. Petrol. Sci. Eng. 145 (2016) 723–733.
[53] S. Shaikh, S.A. Ali, E.Z. Hamad, B.F. Abu-Sharkh, Synthesis and solution properties of poly (acrylamide-styrene) block copolymers with high hydrophobic content, Polym. Eng. Sci. 39 (10) (1999) 1962–1968.
[54] K.C. Dowling, J. Thomas, Photophysical characterization of water-soluble styrene-grafted poly (acrylamide) copolymers, Macromolecules 24 (9) (1991) 2341–2347.
[55] Y.-L. Liu, Y.-H. Chang, W.-H. Chen, Preparation and self-assembled toroids of amphiphilic polystyrene-C60-poly (N-isopropylacrylamide) block copolymers, Macromolecules 41 (21) (2008) 7857–7862.
[56] R.Y. Suckeveriene, R. Rahman, I. Shtein, N. Kharlamova, M. Narkis, Synthesis of styrene–acrylamide copolymer by surfactant-free sonicated dynamic interfacial polymerization, Polym. Adv. Technol. 23 (12) (2012) 1536–1542.
[57] L. Minsk, C. Kotlarchik, G. Meyer, Copolymerization of acrylamide and styrene. II. Reactivity ratios with unperturbed acrylamide, J. Polym. Sci.: Polym. Chem. Ed. 11 (12) (1973) 3037–3042.
[58] Y. Tamsilian, A.R. SA, M. Shaban, S. Ayatollahi, J.C. de la Cal, J.J. Sheng, et al., Nanostructured particles for controlled polymer release in enhanced oil recovery, Energy Technol. 4 (9) (2016) 1035–1046.
[59] H. Khakpour, M. Abdollahi, Synthesis, characterization, rheological properties and hydrophobic nano-association of acrylamide/styrene and acrylamide/sodium styrene sulfonate/styrene co-and terpolymers, J. Polym. Res. 23 (8) (2016) 168.
[60] M. Antoniv, S. Chang, N. Al-Jabri, S.S. Zhu, Surfactant-free synthesis of poly (styrene-co-acrylamide) monodisperse nanoparticles using hybrid flow-to-batch chemistry, J. Appl. Polym. Sci. 138 (9) (2021) 49905.
[61] S. Ghaderi, S.A.A. Ramazani, S.A. Haddadi, Synthesis and characterization of highly hydrophilic self-associating terpolymers: Rheological, thermal, and corrosion protection studies, Chem. Eng. J. 405 (2021), 126939.
[62] A. Maghsoudian, A. Esfandiarian, S. Kord, Y. Tamsilian, B.S. Soulgani, Direct insights into the micro and macro scale mechanisms of symbiotic effect of SO42−, Mg2+, and Ca2+ ions concentration for smart waterflooding in the carbonated coated micromodel system 113700 J. Mol. Liq. (2020).
[63] Y. Tamsilian, A.R. Sa, M. Shaban, S. Ayatollahi, R. Tomovska, High molecular weight polyacrylamide nanoparticles prepared by inverse emulsion polymerization: reaction conditions-properties relationships, Colloid Polym. Sci. 294 (3) (2016) 513–525.
[64] D. Bu, X. Hu, Z. Yang, X. Yang, W. Wei, M. Jiang, et al., Elucidation of the Relationship between Intrinsic Viscosity and Molecular Weight of Cellulose Dissolved in Tetra-N-Butyl Ammonium Hydroxide/Dimethyl Sulfoxide, Polymers 11 (10) (2019) 1605.
[65] M.A. Haruna, D. Wen, Stabilization of Polymer Nanocomposites in High-Temperature and High-Salinity Brines, ACS Omega 4 (7) (2019) 11631–11641.

[66] M. Shirazi, J. Farzaneh, S. Kord, Y. Tamsilian, Smart water spontaneous imbibition into oil-wet carbonate reservoir cores: Symbiotic and individual behavior of potential determining ions, J. Mol. Liq. 299 (2020) 112102.
[67] R. Saha, R.V. Uppaluri, P. Tiwari, Silica nanoparticle assisted polymer flooding of heavy crude oil: emulsification, rheology, and wettability alteration characteristics, Ind. Eng. Chem. Res. 57 (18) (2018) 6364–6376.
[68] M. Ershadi, M. Alaei, A. Rashidi, A. Ramazani, S. Khosravani, Carbonate and sandstone reservoirs wettability improvement without using surfactants for Chemical Enhanced Oil Recovery (C-EOR), Fuel 153 (2015) 408–415.
[69] S. Mohammadi, S. Kord, J. Moghadasi, An experimental investigation into the spontaneous imbibition of surfactant assisted low salinity water in carbonate rocks, Fuel 243 (2019) 142–154.
[70] W. Song, F. Ogunbanwo, M. Steinsbø, M.A. Fernø, A.R. Kovscek, Mechanisms of multiphase reactive flow using biogenically calcite-functionalized micromodels, Lab Chip 18 (24) (2018) 3881–3891.
[71] M.H. Sedaghat, M.H. Ghazanfari, M. Masihi, D. Rashtchian, Experimental and numerical investigation of polymer flooding in fractured heavy oil five-spot systems, J. Petrol. Sci. Eng. 108 (2013) 370–382.
[72] M. Sedaghat, O. Mohammadzadeh, S. Kord, I. Chatzis, Heavy oil recovery using ASP flooding: A pore-level experimental study in fractured five-spot micromodels, Can. J. Chem. Eng. 94 (4) (2016) 779–791.
[73] B. Abedi, M.H. Ghazanfari, R. Kharrat, Experimental study of polymer flooding in fractured systems using five-spot glass micromodel: the role of fracture geometrical properties, Energy Explor. Exploit. 30 (5) (2012) 689–705.
[74] W. Song, A.R. Kovscek, Functionalization of micromodels with kaolinite for investigation of low salinity oil-recovery processes, Lab Chip 15 (16) (2015) 3314–3325.
[75] M.J. Barnaji, P. Pourafshary, M.R. Rasaie, Visual investigation of the effects of clay minerals on enhancement of oil recovery by low salinity water flooding, Fuel 184 (2016) 826–835.
[76] O. Mohammadzadeh, M.H. Sedaghat, S. Kord, S. Zendehboudi, J.P. Giesy, Pore-level visual analysis of heavy oil recovery using chemical-assisted waterflooding process–Use of a new chemical agent, Fuel 239 (2019) 202–218.
[77] L.T. Chiem, L. Huynh, J. Ralston, D.A. Beattie, An in situ ATR–FTIR study of polyacrylamide adsorption at the talc surface, J. Colloid Interface Sci. 297 (1) (2006) 54–61.
[78] S. Karthikeyan, C. Anandan, J. Subramanian, G. Sekaran, Characterization of iron impregnated polyacrylamide catalyst and its application to the treatment of municipal wastewater, RSC Adv. 3 (35) (2013) 15044–15057.
[79] A.-Y. León-Bermúdez, R. Salazar, Synthesis and characterization of the polystyrene-asphaltene graft copolymer by FT-IR spectroscopy, CT&F-Ciencia, Tecnología y Futuro 3 (4) (2008) 157–167.
[80] A. Al-Sabagh, N. Kandile, R. El-Ghazawy, M.N. El-Din, E. El-Sharaky, Synthesis and characterization of high molecular weight hydrophobically modified polyacrylamide nanolatexes using novel nonionic polymerizable surfactants, Egypt. J. Pet. 22 (4) (2013) 531–538.
[81] L. Gaabour, Spectroscopic and thermal analysis of polyacrylamide/chitosan (PAM/CS) blend loaded by gold nanoparticles, Results Phys. 7 (2017) 2153–2158.
[82] F. Candau, J. Selb, Hydrophobically-modified polyacrylamides prepared by micellar polymerization, Adv. Colloid Interface Sci. 79 (2–3) (1999) 149–172.
[83] J. Jung, J. Jang, J. Ahn, Characterization of a polyacrylamide solution used for remediation of petroleum contaminated soils, Materials 9 (1) (2016) 16.
[84] P. Ahmadi, B. Shahsavani, M.R. Malayeri, M. Riazi, Impact of different injection sites on the water and oil exchange in a fractured porous medium for different polymers: A visual study, J. Petrol. Sci. Eng. 174 (2019) 948–958.
[85] N. Lai, W. Dong, Z. Ye, J. Dong, X. Qin, W. Chen, et al., A water-soluble acrylamide hydrophobically associating polymer: Synthesis, characterization, and properties as EOR chemical, J. Appl. Polym. Sci. 129 (4) (2013) 1888–1896.
[86] H. Khakpour, M. Abdollahi, A. Nasiri, Synthesis, microstructural characterization and hydrophobic intermolecular nano-aggregation behavior of acrylamide/2-acrylamido-2-methy-1-propane sulfonic acid/butyl acrylate co-and terpolymers, J. Polym. Res. 22 (10) (2015) 189.
[87] J. Ma, P. Cui, L. Zhao, R. Huang, Synthesis and solution behavior of hydrophobic association water-soluble polymers containing arylalkyl group, Eur. Polym. J. 38 (8) (2002) 1627–1633.
[88] A. Rahimi, B. Honarvar, M. Safari, The role of salinity and aging time on carbonate reservoir in low salinity seawater and smart seawater flooding, J. Petrol. Sci. Eng. 187 (2020) 106739.
[89] A. Rahimi, M. Safari, B. Honarvar, H. Chabook, R. Gholami, On time dependency of interfacial tension through low salinity carbonated water injection, Fuel 280 (2020) 118492.
[90] M. Safari, A. Rahimi, R. Gholami, A. Permana, Khur W. Siaw, Underlying mechanisms of shale wettability alteration by low salinity water injection (LSWI), J. Dispersion Sci. Technol. (2020) 1–9.
[91] B. Honarvar, A. Rahimi, M. Safari, S. Khajehahmadi, M. Karimi, Smart water effects on a crude oil-brine-carbonate rock (CBR) system: further suggestions on mechanisms and conditions, J. Mol. Liq. 299 (2020) 112173.
[92] M. Safari, A. Rahimi, R.M. Lah, R. Gholami, W.S. Khur, Sustaining sulfate ions throughout smart water flooding by nanoparticle based scale inhibitors, J. Mol. Liq. 310 (2020) 113250.
[93] B. Honarvar, A. Rahimi, M. Safari, S. Rezaee, M. Karimi, Favorable attributes of low salinity water aided alkaline on crude oil-brine-carbonate rock system, Colloids Surf., A 585 (2020) 124144.
[94] A. Piroozian, M. Hemmati, M. Safari, A. Rahimi, O. Rahmani, S.M. Aminpour, et al., A mechanistic understanding of the water-in-heavy oil emulsion viscosity variation: effect of asphaltene and wax migration, Colloids Surf., A 608 (2021) 125604.
[95] A. Esfandiarian, A. Maghsoudian, M. Shirazi, Y. Tamsilian, S. Kord, J.J. Sheng, Mechanistic Investigation of the Synergy of a Wide Range of Salinities and Ionic Liquids for Enhanced Oil Recovery: Fluid-Fluid Interactions, Energy Fuels 35 (4) (2021) 3011–3031.
[96] R. Guzmán, J. Ancheyta, F. Trejo, S. Rodríguez, Methods for determining asphaltene stability in crude oils, Fuel 188 (2017) 530–543.
[97] I. Ismail, Y. Kazemzadeh, M. Sharifi, M. Riazi, M.R. Malayeri, F. Cortés, Formation and stability of W/O emulsions in presence of asphaltene at reservoir thermodynamic conditions, J. Mol. Liq. 299 (2020) 112125.